

Records of Punctuated Tectonism in Platform-Interior Graben Systems (Ontario, Canada) Far-Flung from Contemporaneous Taconic Orogenesis in the Northern Appalachians

Sajal Sharma¹, George R. Dix², Mario Coniglio³, Aicha Achab⁴, and John F. V. Riva⁴. (1) AGAT Laboratories Ltd., 3801 21 St N.E., Calgary, AB T2E 6T5, Canada, phone 403-6806292, email-sharma@agatlabs.com. (2) Department of Earth Sciences, Carleton University, 1125 Colonel By Drive, Ontario, ON K1S 5B6, Canada. (3) University of Waterloo. (4) INRS-ETE, Université du Québec, Québec, QC, Canada.

Abstract

Ordovician basins along the craton-interior of the Ottawa-Bonnechère and Temiskaming graben systems of eastern and northern Ontario, respectively, form an interconnected structural corridor (up to 600 km in length) extending northwest of the Taconic Orogen. Both graben systems preserve cryptic evidence of Late Ordovician tectonic events far-flung from the present structural limits of the orogen, events that help define the changing regional influence and patterns of foreland basin development. In both graben systems, collapse of a regional carbonate platform and formation of local deep-water shale basins occurred by ~452 Ma. In the Ottawa-Bonnechère graben, in eastern Ontario, a K-bentonite punctuates deposition of organic-rich shales within the *pygmæus* graptolite Biozone (~451 to 452 Ma). It immediately precedes the onset of distal turbidity flows and, unlike older platform-hosted K-bentonites in eastern North America, its geochemistry identifies greater incorporation of continental crust within the magmatic source. Whether the bentonite is either regional in extent or is a more local basin-restricted eruptive is uncertain, but its composition and timing suggests it was linked to fundamental changes in Taconic basin architecture. Within the Temiskaming graben, a seafloor hydrothermal event is recorded within slightly younger shales (*manitoulinensis* graptolite Biozone; ~449-451 Ma) by a microfossil-rich (conodont, chitinozoan) phosphatic sandy-shale, which contains rare (<5%) fluorite and common (~60%) microcrystalline ferroan dolomite. Hydrothermal fluids briefly stimulated productivity, and likely arose along basement faults controlled by Taconian crustal stress. Hydrothermal activity may help explain some dolomitization of Ordovician and Silurian strata in this basin.

INTRODUCTION

Ordovician basins along the craton-interior of the Ottawa-Bonnechère and Temiskaming graben systems of eastern and northern Ontario, respectively, form an interconnected structural corridor (up to 600 km in length) extending northwest of the Taconic Orogen (Fig. 1). Both graben systems preserve cryptic evidence of Late Ordovician tectonic events far-flung from the present structural limits of the orogen, events that help define the changing regional influence and patterns of foreland basin development. In both graben systems, collapse of a regional carbonate platform and formation of local deep-water shale basins occurred by ~452 Ma (Figs. 2 and 7). In eastern Ontario, the Lindsay Formation defines the top of the carbonate platform, and is overlain by deep-water basinal mudrock of the Billings Formation (Fig. 2), and then by Taconic flysch of the Carlsbad Formation. In northern Ontario, the Farr Formation records the top of the carbonate platform, and is overlain by basinal shale of Dawson Point Formation (Fig. 7). We examine two tectonic events that are preserved within the post-platform shale basins in both graben systems, recorded in the Geological Survey of Canada Russell No. 2, and the Ontario Geological Survey, LT-1drill cores.

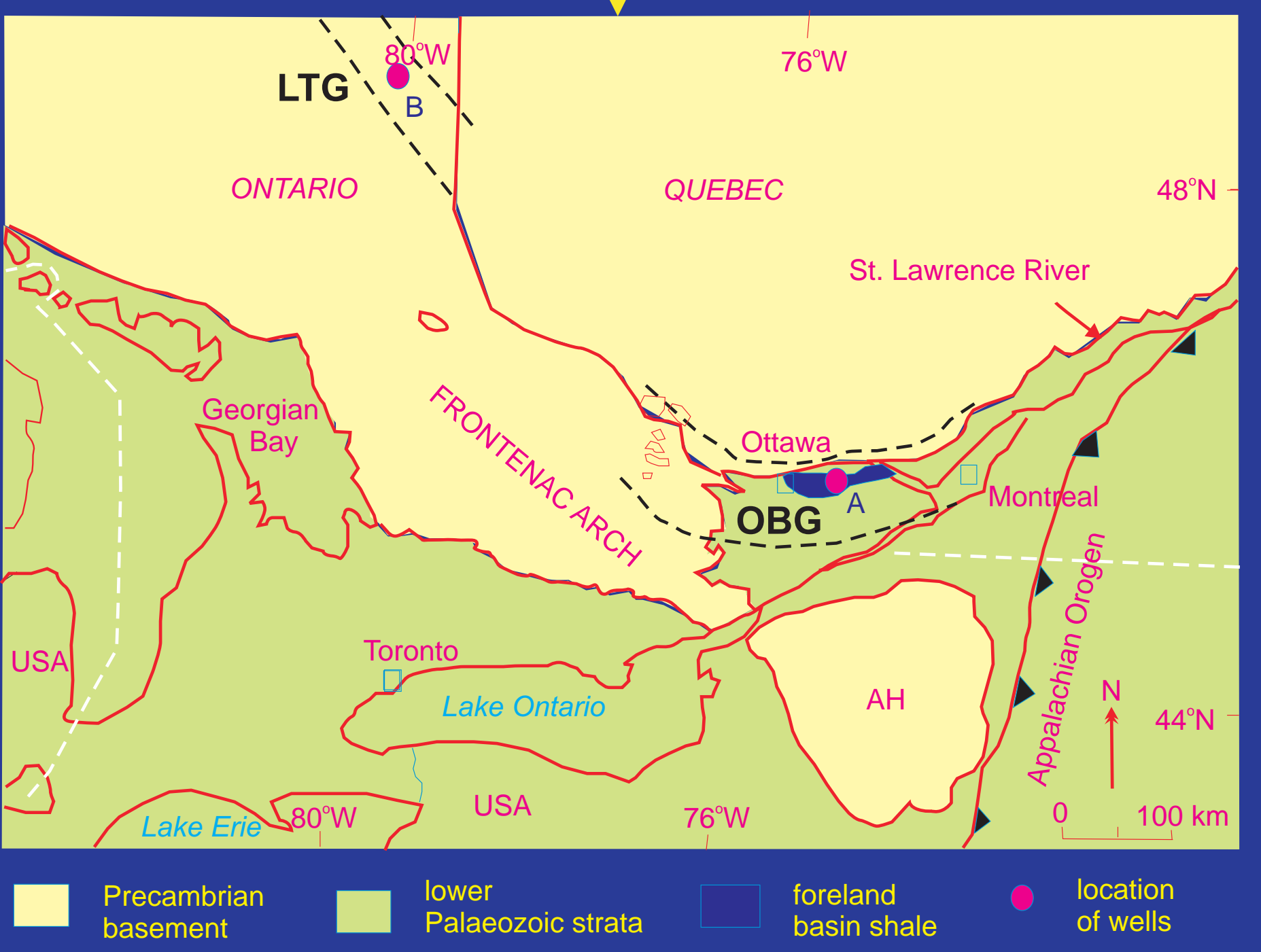


Figure 1. Regional bedrock geology of southern Ontario, showing locations of drill cores A and B from the Ottawa Bonnechère Graben (OBG) and Lake Temiskaming Graben (LTG), respectively. AH = Adirondack Highlands. Modified from Sharma et al. (2003) and Williams et al. (1992).

RUSSELL K-BENTONITE; IMPLICATIONS FOR TACONIAN BASIN EVOLUTION IN EASTERN ONTARIO

In the Ottawa-Bonnechère graben (Fig. 1), a K-bentonite (Russell K-bentonite) punctuates deposition of organic-rich shales within the *pygmæus* graptolite Biozone (~451 to 452 Ma). Although some K-bentonites have been reported from this interval in eastern North America, compositional data is available only for the Russell K-bentonite. Gamma-log correlation suggests a potential minimum distribution area of <2x10³ km² for the bed covering part of southern Quebec, New York State, and eastern Ontario (Figure 2). The deposit immediately precedes the first influx of distal turbidites into this shale basin, associated with Taconic flysch and simultaneous abrupt ventilation of this once anoxic deep-water basin, which formed initially after foundering of the Upper Ordovician carbonate platform. Concurrent intrabasinal extinction of several graptolite species suggests that change in sedimentation, paleoceanography and volcanism were linked to a regional external process (Sharma et al., 2003).

The Russell K-bentonite is distinct from the older (better known) Ordovician platform ash bed in eastern North America in many aspects. It contains abundant titaniferous phlogopite with 1.6 % BaO, fluorapatite with 2.5% F, and dynamically shaped glass spherules now altered to clay (Figure 3). The spherules and clay matrix constitute 45 % of the bed, and, compositionally, define an illite (>90%) smectite (I/S) structure with about 7.5 % K₂O. Age-date by laser Ar-Ar analysis of the phlogopite crystals yielded a younger than expected (440-445 Ma) age (Figure 4). The magmatic source of the Russell K-bentonite falls within the trachyanidesite field, and was Ba-enriched.

Comparison of geochemistry and mineralogy of Russell Bed with older, Middle to Late Ordovician and younger Early Silurian K-bentonites within the Taconic orogen along eastern Laurentia and Baltica identifies that the potential source magma for the bed was more mafic, alkaline, and less fractionated than sources typical of the older, platform-hosted bentonites. Instead, it is compositionally more similar to the younger Llandovery bentonites of Scandinavia and Scotland (Fig. 5). Whether the bentonite is of regional extent or is a more local basin-restricted eruptive remains uncertain, but its composition and timing suggests it was linked to fundamental changes in source magma coincidental with change in basin architecture.

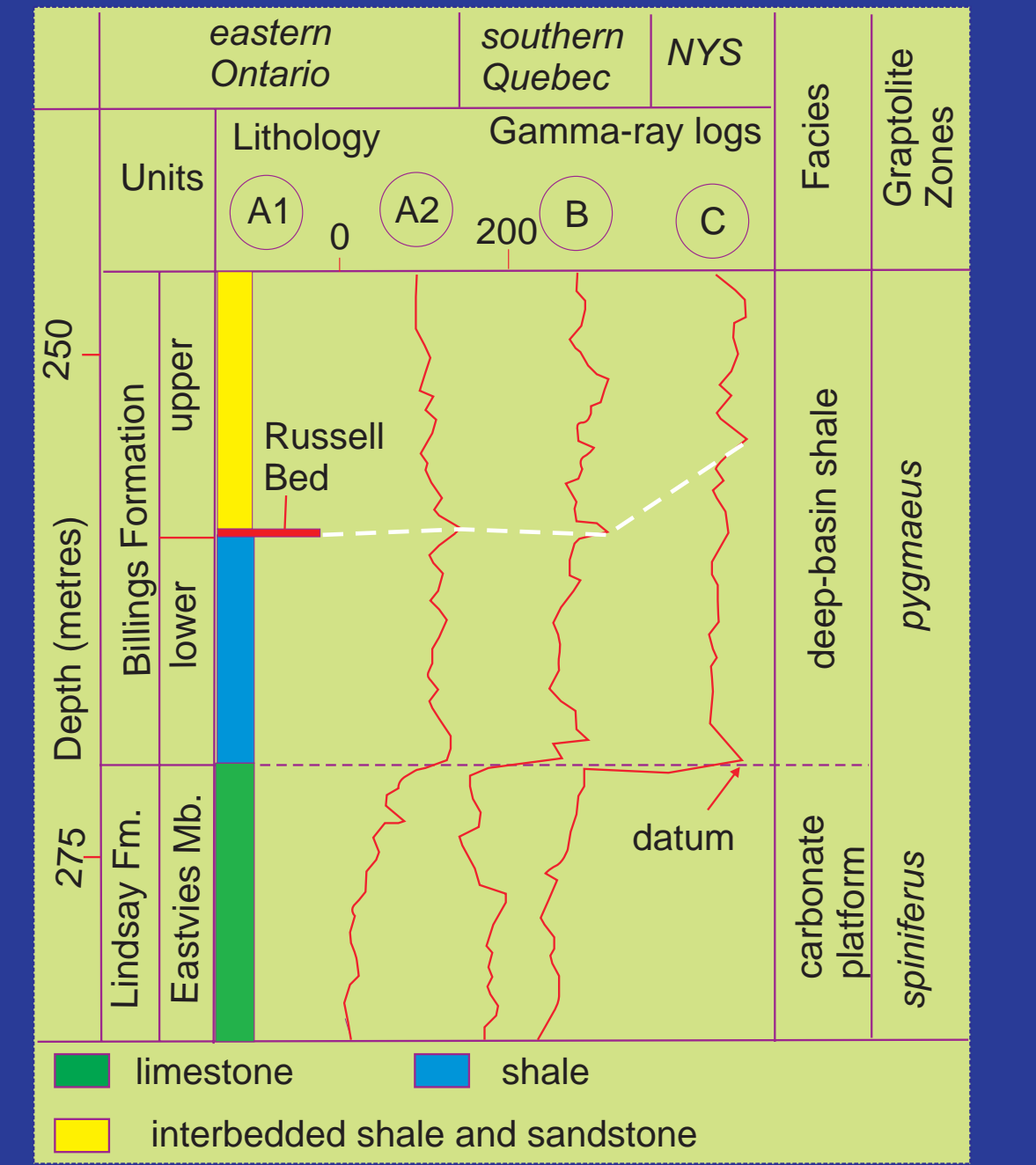


Figure 2. Lithostratigraphy and graptolite biostratigraphy from sites in eastern Ontario (A). Gamma-ray logs from southern Quebec (B) and New York State (C) showing likely correlative distribution of the K-bentonite (after Sharma et al., 2005).

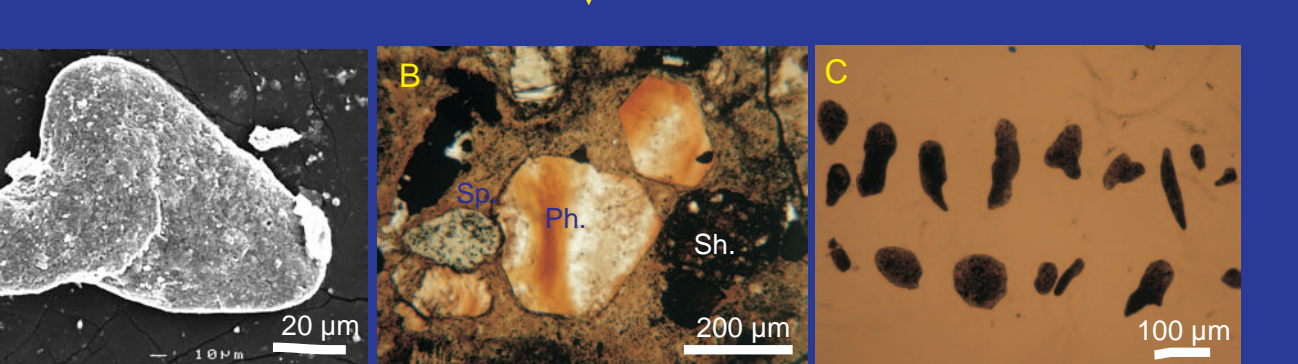


Figure 3. (A) An altered glass spherule under SEM. (B) Thin section photomicrograph showing phlogopite phenocryst (Ph), altered glass spherule (Sp.) and fragment of a shale (Sh.). (C) Altered glass spherules mounted on a thin section under reflected light.

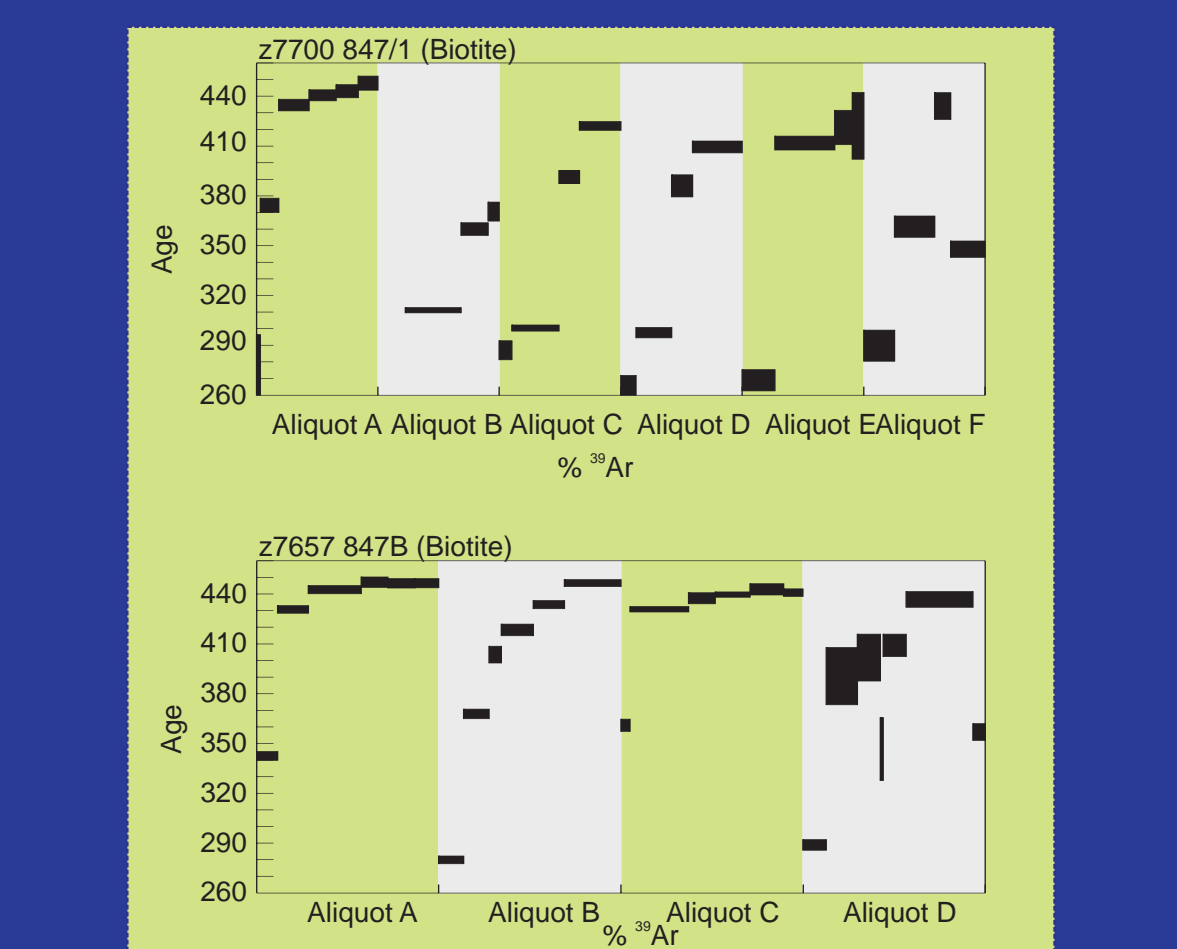


Figure 4. Laser Ar-Ar data for biotite phenocrysts from the Russell Bed.

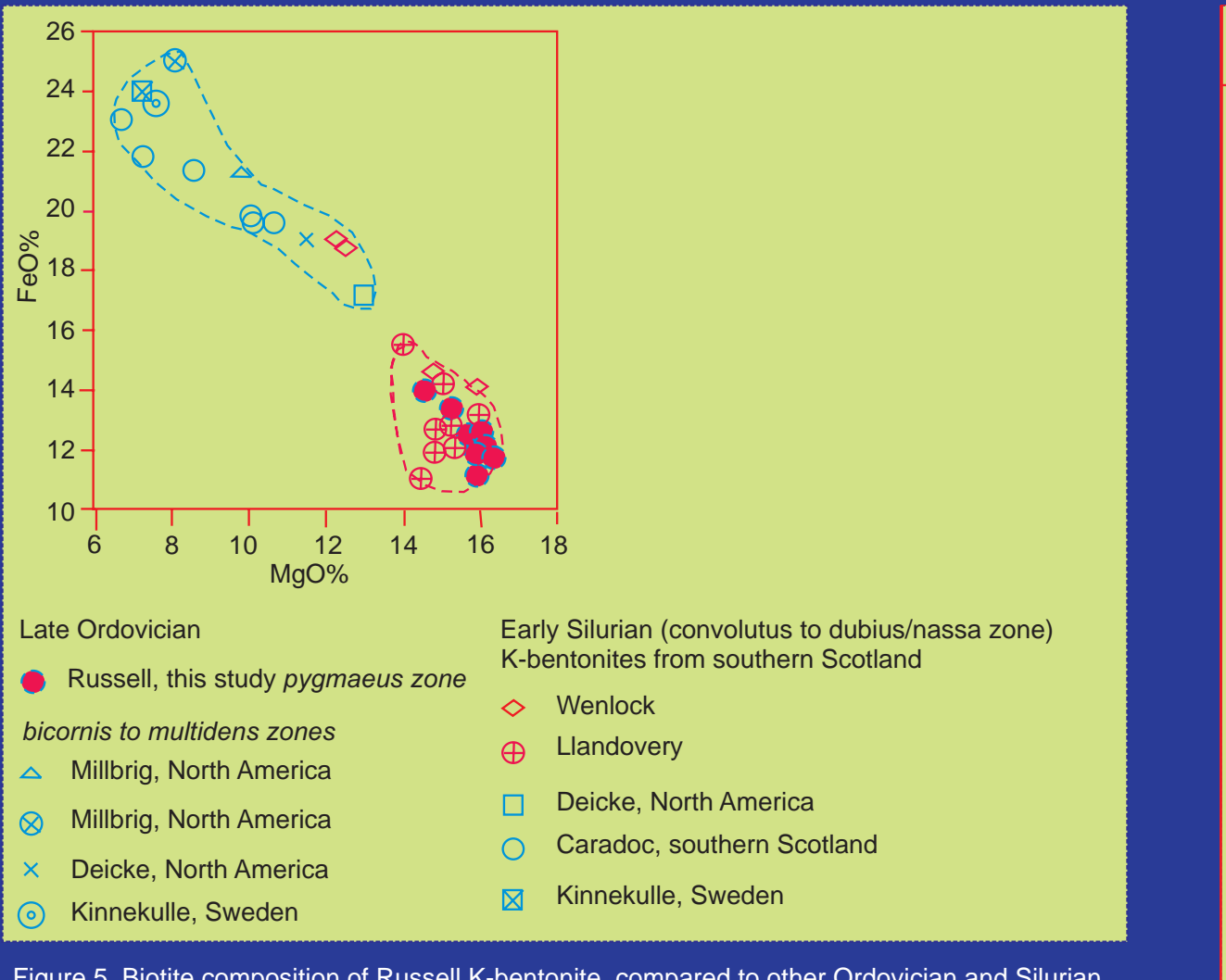


Figure 5. Biotite composition of Russell K-bentonite, compared to other Ordovician and Silurian K-bentonites from North America and Baltica (modified after Sharma et al., 2005).

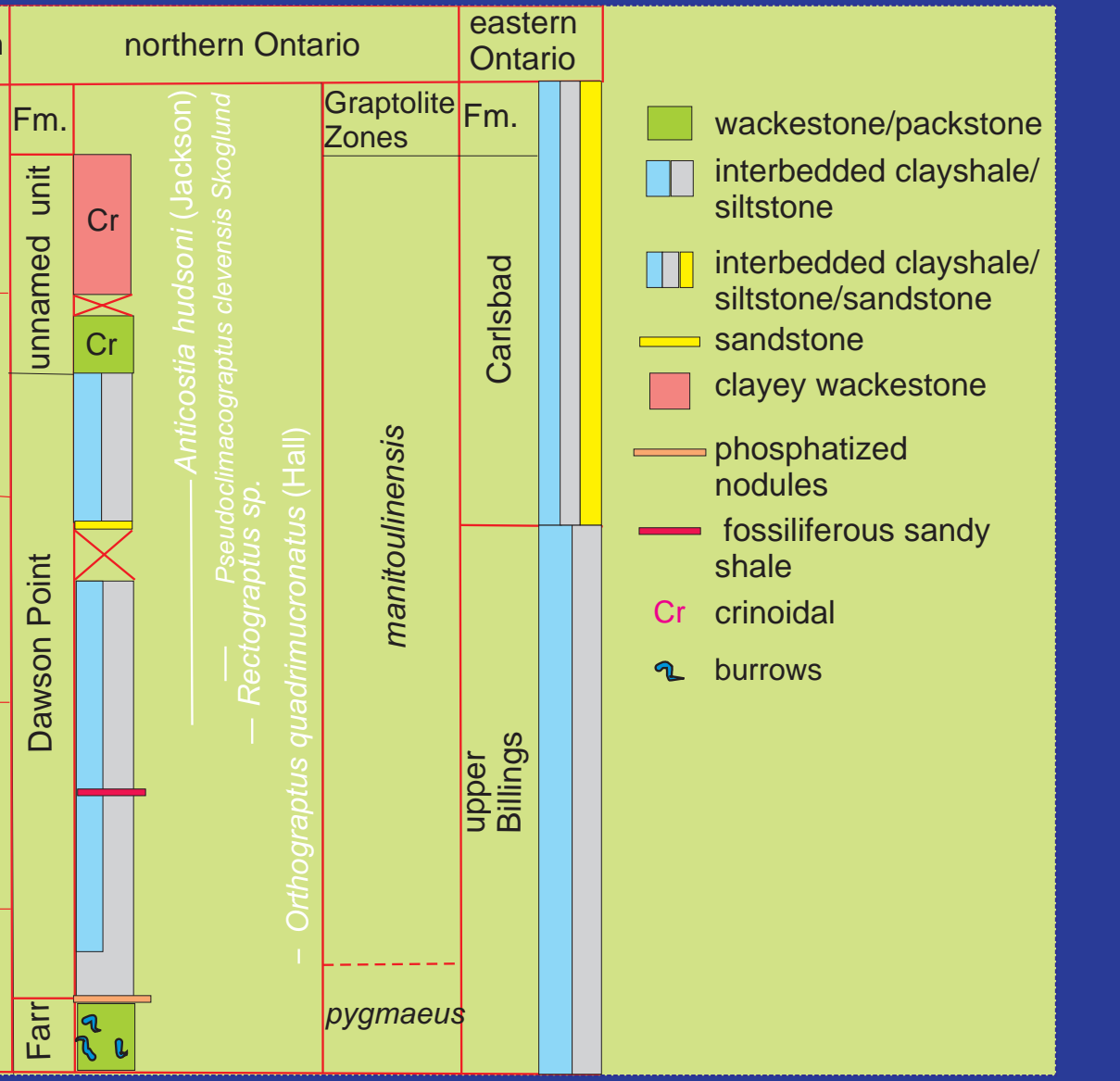


Figure 6. Lithostratigraphy and graptolite biostratigraphy of the core from Temiskaming, northern Ontario, compared to the deep-basinal shale succession in eastern Ontario.

SEAFLOOR HYDROTHERMAL DOLOMITIZATION, TEMISKAMING GRABEN
Within the Temiskaming Graben, a fossil-rich (conodont, chitinozoan, gastropod, bivalve) phosphatic sandy-shale with abundant dolomites (Figure 6) is recorded within slightly younger (*manitoulinensis* graptolite Biozone; ~449-451 Ma; Figure 7) in the deep-basinal shales encountered in the LT-1 core.

Biostratigraphy

Fossils were recovered from several levels in the LT-1drill core, which traversed the Dawson Point Formation (Figure 7).

The graptolites from the 119-132 m interval mainly belong to two (2) species: *Pseudoclimacograptus clevensis* Skoglund and *Arnhemograptus anacanthus* (Mitchell & Bergström), which are indicative of the upper *manitoulinensis* graptolite Zone (Figure 8). The long-ranging *Orthograptus quadrifurcatus* (Hall) was also recovered from the lower 142 m level (Figure 7).

Biostrophigraphy
Fossils were recovered from several levels in the LT-1drill core, which traversed the Dawson Point Formation (Figure 7).

The graptolites from the 119-132 m interval mainly belong to two (2) species:

Pseudoclimacograptus clevensis Skoglund and *Arnhemograptus anacanthus* (Mitchell & Bergström), which are indicative of the upper *manitoulinensis* graptolite Zone (Figure 8). The long-ranging *Orthograptus quadrifurcatus* (Hall) was also recovered from the lower 142 m level (Figure 7).

Pyritized chitinozoans associated with small gastropods and bryozoans were recovered from the core from 133 m level. They consist of internal molds and, in some cases, remnants of the chitinozoan external wall and its ornamentation. Three (3) genera have been recognized: *Conochitina*, *Cyathochitina* and *Hercoclitina* (Figure 9). Although the state of preservation does not allow for a precise determination, the association is indicative of a late Ordovician age.

Fragments of conodonts that were recovered from the core at 133 m level are: *Amorphognathus* sp. indet. - 5, *Drepanoistodus subrectus* (Branson and Mehl) - 2, *Panderodus gracilis* (Branson and Mehl) - 2, *Pariostodus nowlani* Zhen, Webby and Barnes - 1, *Phragmodus undatus* Branson and Mehl - 4, *Plectiodus* sp. indet. - 4 (written communication, Dr. Godfrey Nowlan, Geological Survey of Canada, Calgary). The fragmentary nature of the specimens does not allow a definitive age for the sample. The sample could be of late Middle to Late Ordovician in age. The specimens are difficult to assess for colour alteration index because there is detritus in the basal cavities of many specimens and most specimens show some signs of abrasion.

Careful comparison of several specimens with CAI standards on a white background leads to conclude that they are altered only slightly and have a value of 1.5.

This fossiliferous, shale bed contains rare (<5%) fluorite and common (~60%) microcrystalline ferroan dolomite (FeO= 5.04±0.36) dolomite (Fig. 6). δ¹⁸O (-4.83±0.02 PDB; n=5) and δ¹³C (0.68±0.04 PDB, n=5) suggests a relatively heavier isotopic composition compared to dolomites typical of the underlying local and regional carbonate platform (Fig. 10). Two dolomite samples analyzed from the carbonate platform from the Temiskaming area also indicate a depleted composition (δ¹⁸O, -6.11 to -6.57 PDB and δ¹³C, -0.08 to -0.28 PDB) relative to the dolomites of the shale bed. ⁸⁷Sr/⁸⁶Sr values from the dolomites within the shale varies from 0.709034 to 0.71037 (Figure 11).

This fossiliferous, shale bed contains rare (<5%) fluorite and common (~60%) microcrystalline ferroan dolomite (FeO= 5.04±0.36) dolomite (Fig. 6). δ¹⁸O (-4.83±0.02 PDB; n=5) and δ¹³C (0.68±0.04 PDB, n=5) suggests a relatively heavier isotopic composition compared to dolomites typical of the underlying local and regional carbonate platform (Fig. 10). Two dolomite samples analyzed from the carbonate platform from the Temiskaming area also indicate a depleted composition (δ¹⁸O, -6.11 to -6.57 PDB and δ¹³C, -0.08 to -0.28 PDB) relative to the dolomites of the shale bed. ⁸⁷Sr/⁸⁶Sr values from the dolomites within the shale varies from 0.709034 to 0.71037 (Figure 11).

This fossiliferous, shale bed contains rare (<5%) fluorite and common (~60%) microcrystalline ferroan dolomite (FeO= 5.04±0.36) dolomite (Fig. 6). δ¹⁸O (-4.83±0.02 PDB; n=5) and δ¹³C (0.68±0.04 PDB, n=5) suggests a relatively heavier isotopic composition compared to dolomites typical of the underlying local and regional carbonate platform (Fig. 10). Two dolomite samples analyzed from the carbonate platform from the Temiskaming area also indicate a depleted composition (δ¹⁸O, -6.11 to -6.57 PDB and δ¹³C, -0.08 to -0.28 PDB) relative to the dolomites of the shale bed. ⁸⁷Sr/⁸⁶Sr values from the dolomites within the shale varies from 0.709034 to 0.71037 (Figure 11).

This fossiliferous, shale bed contains rare (<5%) fluorite and common (~60%) microcrystalline ferroan dolomite (FeO= 5.04±0.36) dolomite (Fig. 6). δ¹⁸O (-4.83±0.02 PDB; n=5) and δ¹³C (0.68±0.04 PDB, n=5) suggests a relatively heavier isotopic composition compared to dolomites typical of the underlying local and regional carbonate platform (Fig. 10). Two dolomite samples analyzed from the carbonate platform from the Temiskaming area also indicate a depleted composition (δ¹⁸O, -6.11 to -6.57 PDB and δ¹³C, -0.08 to -0.28 PDB) relative to the dolomites of the shale bed. ⁸⁷Sr/⁸⁶Sr values from the dolomites within the shale varies from 0.709034 to 0.71037 (Figure 11).

This fossiliferous, shale bed contains rare (<5%) fluorite and common (~60%) microcrystalline ferroan dolomite (FeO= 5.04±0.36) dolomite (Fig. 6). δ¹⁸O (-4.83±0.02 PDB; n=5) and δ¹³C (0.68±0.04 PDB, n=5) suggests a relatively heavier isotopic composition compared to dolomites typical of the underlying local and regional carbonate platform (Fig. 10). Two dolomite samples analyzed from the carbonate platform from the Temiskaming area also indicate a depleted composition (δ¹⁸O, -6.11 to -6.57 PDB and δ¹³C, -0.08 to -0.28 PDB) relative to the dolomites of the shale bed. ⁸⁷Sr/⁸⁶Sr values from the dolomites within the shale varies from 0.709034 to 0.71037 (Figure 11).

This fossiliferous, shale bed contains rare (<5%) fluorite and common (~60%) microcrystalline ferroan dolomite (FeO= 5.04±0.36) dolomite (Fig. 6). δ¹⁸O (-4.83±0.02 PDB; n=5) and δ¹³C (0.68±0.04 PDB, n=5) suggests a relatively heavier isotopic composition compared to dolomites typical of the underlying local and regional carbonate platform (Fig. 10). Two dolomite samples analyzed from the carbonate platform from the Temiskaming area also indicate a depleted composition (δ¹⁸O, -6.11 to -6.57 PDB and δ¹³C, -0.08 to -0.28 PDB) relative to the dolomites of the shale bed. ⁸⁷Sr/⁸⁶Sr values from the dolomites within the shale varies from 0.709034 to 0.71037 (Figure 11).

This fossiliferous, shale bed contains rare (<5%) fluorite and common (~60%) microcrystalline ferroan dolomite (FeO= 5.04±0.36) dolomite (Fig. 6). δ¹⁸O (-4.83±0.02 PDB; n=5) and δ¹³C (0.68±0.04 PDB, n=5) suggests a relatively heavier isotopic composition compared to dolomites typical of the underlying local and regional carbonate platform (Fig. 10). Two dolomite samples analyzed from the carbonate platform from the Temiskaming area also indicate a depleted composition (δ¹⁸O, -6.11 to -6.57 PDB and δ¹³C, -0.08 to -0.28 PDB) relative to the dolomites of the shale bed. ⁸⁷Sr/⁸⁶Sr values from the dolomites within the shale varies from 0.709034 to 0.71037 (Figure 11).

This fossiliferous, shale bed contains rare (<5%) fluorite and common (~60%) microcrystalline ferroan dolomite (FeO= 5.04±0.36) dolomite (Fig. 6). δ¹⁸O (-4.83±0.02 PDB; n=5) and δ¹³C (0.68±0.04 PDB, n=5) suggests a relatively heavier isotopic composition compared to dolomites typical of the underlying local and regional carbonate platform (Fig. 10). Two dolomite samples analyzed from the carbonate platform from the Temiskaming area also indicate a depleted composition (δ¹⁸O, -6.11 to -6.57 PDB and δ¹³C, -0.08 to -0.28 PDB) relative to the dolomites of the shale bed. ⁸⁷Sr/⁸⁶Sr values from the dolomites within the shale varies from 0.709034 to 0.71037 (Figure 11).

This fossiliferous, shale bed contains rare (<5%) fluorite and common (~60%) microcrystalline ferroan dolomite (FeO= 5.04±0.36) dolomite (Fig. 6). δ¹⁸O (-4.83±0.02 PDB; n=5) and δ¹³C (0.68±0.04 PDB, n=5) suggests a relatively heavier isotopic composition compared to dolomites typical of the underlying local and regional carbonate platform (Fig. 10). Two dolomite samples analyzed from the carbonate platform from the Temiskaming area also indicate a depleted composition (δ¹⁸O, -6.11 to -6.57 PDB and δ¹³C, -0.08 to -0.28 PDB) relative to the dolomites of the shale bed. ⁸⁷Sr/⁸⁶Sr values from the dolomites within the shale varies from 0.709034 to 0.71037 (Figure 11).

This fossiliferous, shale bed contains rare (<5%) fluorite and common (~60%) microcrystalline ferroan dolomite (FeO= 5.04±0.36) dolomite (Fig. 6). δ¹⁸O (-4.83±0.02 PDB; n=5) and δ¹³C (0.68±0.04 PDB, n=5) suggests a relatively heavier isotopic composition compared to dolomites typical of the underlying local and regional carbonate platform (Fig. 10). Two dolomite samples analyzed from the carbonate platform from the Temiskaming area also indicate a depleted composition (δ¹⁸O, -6.11 to -6.57 PDB and δ¹³C, -0.08 to -0.28 PDB) relative to the dolomites of the shale bed. ⁸⁷Sr/⁸⁶Sr values from the dolomites within the shale varies from 0.709034 to 0.71037 (Figure 11).

This fossiliferous, shale bed contains rare (<5%) fluorite and common (~60%) microcrystalline ferroan dolomite (FeO= 5.04±0.36) dolomite (Fig. 6). δ¹⁸O (-4.83±0.02 PDB; n=5) and δ¹³C (0.68±0.04 PDB, n=5) suggests a relatively heavier isotopic composition compared to dolomites typical of the underlying local and regional carbonate platform (Fig. 10). Two dolomite samples analyzed from the carbonate platform from the Temiskaming area also indicate a depleted composition (δ¹⁸O, -6.11 to -6.57 PDB and δ¹³C, -0.08 to -0.28 PDB) relative to the dolomites of the shale bed. ⁸⁷Sr/⁸⁶Sr values from the dolomites within the shale varies from 0.709034 to 0.71037 (Figure 11).

This fossiliferous, shale bed contains rare (<5%) fluorite and common (~60%) microcrystalline ferroan dolomite (FeO= 5.04±0.36) dolomite (Fig. 6). δ¹⁸O (-4.83±0.02 PDB